

Article

Triangulopteris lacunata gen. et sp. nov. (Centroplasthelida), a New Centrohelid Heliozoan from Soil [†]

Dmitry G. Zagumyonnyi ^{1,2,*} , Liudmila V. Radaykina ² and Denis V. Tikhonenkov ^{1,2} ¹ AquaBioSafe Laboratory, University of Tyumen, 625003 Tyumen, Russia; tikho-denis@yandex.ru² Papanin Institute for Biology of Inland Waters, Russian Academy of Sciences, 152742 Borok, Russia; ld0810@mail.ru

* Correspondence: zdmitryg@gmail.com; Tel.: +7-485-472-4533

[†] <http://zoobank.org/NomenclaturalActs/01EB060E-9DC7-49CF-99CE-71FED936B6F2> and <http://zoobank.org/NomenclaturalActs/4B2D297B-9C53-4160-A49F-79690BEE5719>.

Abstract: A new genus and species of centrohelid heliozoans, *Triangulopteris lacunata* gen. et sp. nov. (Pterocystidae Cavalier-Smith and Heyden, 2007), from four geographically remote locations (the Crimean Peninsula, the Dnieper Lowland (the East European Plain), Franz Josef Land, and the Kolyma Lowland (North–Eastern Siberia) was examined using light and electron microscopy. The novel centrohelid is characterized by round shape, 4.3–16.3 µm in diameter, covered with two types of scales: 1.06–4.54 µm long triangular spine scales and 1.22–2.05 µm oval plate scales. Studied centrohelid heliozoan possesses a unique spine scale morphology. The base of scales is represented by a horse hoof-shaped basal plate. The inner surface and lateral wings of spine scales have numerous radial ribs with two ‘pockets’ that are located on both sides of the spine shaft. These pockets are formed by the lateral wings and ends of the basal plate. The cyst formation and transition to a spicules-bearing stage were noted. Additionally, phylogenetic tree was constructed based on SSU rRNA sequences including the strain HF-25 from the permafrost of Kolyma Lowland. The resulting phylogeny recovered it within the clade Pterista, while forming a separate sister lineage to H2 clade, which only had included freshwater environmental sequences.

Keywords: protists; centrohelid heliozoans; *Triangulopteris lacunata*; morphology; skeletal elements; electron microscopy; 18S rDNA



Citation: Zagumyonnyi, D.G.; Radaykina, L.V.; Tikhonenkov, D.V. *Triangulopteris lacunata* gen. et sp. nov. (Centroplasthelida), a New Centrohelid Heliozoan from Soil. *Diversity* **2021**, *13*, 658. <https://doi.org/10.3390/d13120658>

Academic Editors: Michael Wink, Boris A. Levin and Yulia V. Bespalaya

Received: 15 November 2021

Accepted: 8 December 2021

Published: 11 December 2021

Publisher’s Note: MDPI stays neutral with regard to jurisdictional claims in published maps and institutional affiliations.



Copyright: © 2021 by the authors. Licensee MDPI, Basel, Switzerland. This article is an open access article distributed under the terms and conditions of the Creative Commons Attribution (CC BY) license (<https://creativecommons.org/licenses/by/4.0/>).

1. Introduction

Centrohelid heliozoans (Centroplasthelida Febvre-Chevalier et Febvre, 1984) are a group of free-living heterotrophic protists, found throughout global marine and freshwaters bodies, and soils [1]. Based on multigene phylogeny, centrohelids form a eukaryotic supergroup, Haptista, along with haptophytes [2]. The characteristic features of centrohelids are a peculiar organization of the microtubule-organizing center (MTOC), extrusive organelles (kinetocysts), ribbon-like cristae of mitochondria, narrow pseudopodia (axopodia) with a complex arrangement of microtubule inside, and external skeletal elements [1,3–6]. Most centrohelids are covered with various types of silica scales and/or organic needle-like spicules and the morphology of these coverings have been used to distinguish different genera and species. However, several centrohelid genera can lose silica scales and produce radial needle-shaped organic spicules in clonal cultures [7,8] making morphology-based species identification more challenging.

Described representatives of this group have various cell sizes, from 3 µm in *Choanocystis minima* Zlatogursky, 2010 to 150 µm in *Acanthocystis turfacea* Carter, 1863, which allows them to occupy different niches in microbial food webs. Centrohelids feed on bacteria [9], small heterotrophic flagellates, unicellular algae, ciliates, and even small multicellular organisms [1,6]. Centrohelids also occupy diverse biotopes, ranging from plankton, benthos and periphyton communities of freshwater to hyperhaline environment [1,6,10,11].

However, most studies on centrohelid heliozoans are focused on ones found in freshwater. Specifically, reports on diversity and abundance of centrohelids from soil biotopes are handful [12,13]. Rather, soil biotopes were discarded as unsuitable habitats for centrohelids due to frequent changes in moisture level [1]. There are only a few works that mention centrohelids in soil samples [12,13]. On the contrary, modern metabarcoding investigations show that soil centrohelids are numerous and even more diverse than marine and freshwater ones [14,15].

To date, about 130 morphospecies of centrohelid heliozoans are characterized. Based on 18S rRNA gene sequencing of cultured strains and environmental sequences, it was suggested that the 130 morphospecies represent only 10% of the centrohelid diversity to date [12]. This assumption seems reasonable, since a lot of new species, genera and families of centrohelids were described over the past years [9,12,16–29].

Despite the ubiquity of centrohelids across various ecological niches, very little is known about their biogeography [27,30]. In this study, to better understand the diversity, ecology and phylogeny of this group, in depth morphological investigation was carried out using light and electron microscopy and a molecular phylogenetic analysis. Furthermore, centrohelids from different types of soil biotopes were obtained and clone-cultured for a detailed investigation of the life cycles.

Here, we describe the novel *Triangulopteris lacunata* gen. et sp. nov., a representative of the Pterista lineage.

2. Materials and Methods

2.1. Clone Isolation

Samples were obtained from geographically distant biotopes of the Crimean Peninsula, the Dnieper Lowland (East European Plain), Franz Josef Archipelago and the Kolyma Lowland (North–Eastern Siberia) (see Table 1 and Figure 1).

Table 1. Description of sampling sites.

No	Sampling Site	Date	Biotope	Coordinates
1	Syuryu-Kaya Mt, Crimean Peninsula	14 August 2016	Soil of dry stream	44°56′07.8″ N 35°12′38.7″ E
2	Pesiv Island, Dnieper Lowland, East European Plain	11 October 2014	Soil and willow leaf litter	50°30′14.68″ N 30°31′57.16″ E
3	Champ Island (Franz Josef Land archipelago, Arctic Ocean)	6 August 2019	Moss with sand in the glacier melting zone (70 m from water edge), polar desert	80°37′46.8″ N 56°53′45.5″ E
4	Cape Maliy Chukochiy vicinity, Kolyma Lowland (North–Eastern Siberia)	August 2016	Buried peat, cryoturbated soil from 40 cm depth and mineral soil from 65 depth	70°03′53.9″ N 159°44′06.6″ E

Soil samples were placed into 15 or 50 mL plastic tubes and kept at 4 °C until processed in a laboratory. Each sample was processed by diluting with autoclaved mineral water (Aqua Minerale, PepsiCo, Inc., Moscow oblast, Russia). The diluted samples were then plated onto plastic or glass Petri dish (60 mm in diameter), enriched with a suspension of *Pseudomonas fluorescens* Migula, 1895 bacteria or an autoclaved grain of rice.

The processed samples were kept at 22 °C in the dark and observed for 10 days to reveal the hidden species diversity [31]. To obtain clonal cultures, the individual heliozoan cells were transferred using a glass micropipette onto Petri dish containing a clonal culture of eukaryotic prey. The prey cultures of flagellates *Parabodo caudatus* (Dujardin 1841) Moreira et al., 2004 (strain BAS-1, IBIW RAS) or *Bodo saltans* Ehrenberg 1832 (strain PI-1, IBIW RAS) were grown in mineral water (Aqua Minerale, PepsiCo, Inc., Moscow oblast, Russia).

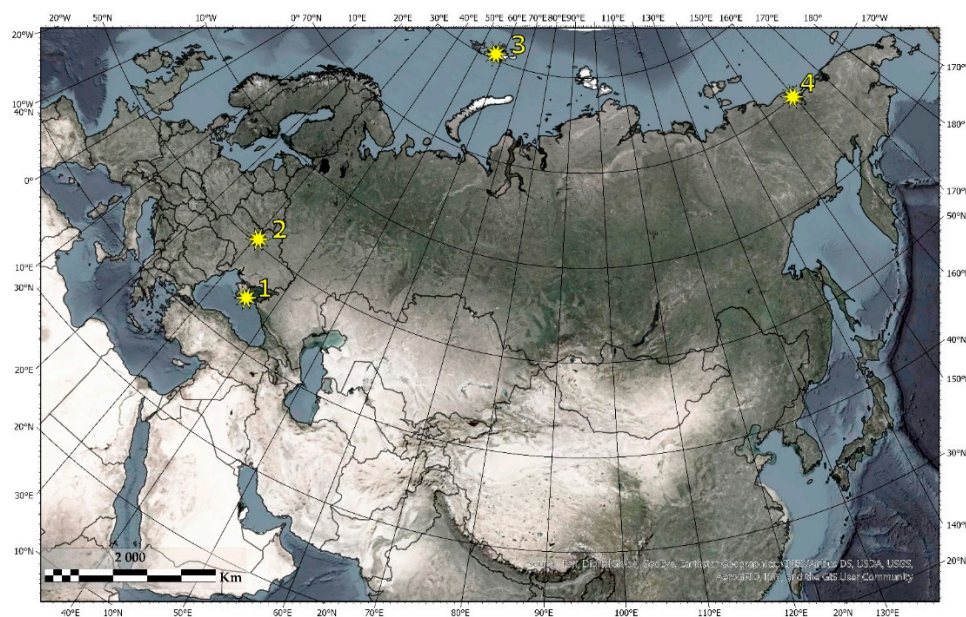


Figure 1. Map of sampling sites. See Table 1 for the description of the sampling sites (1–4).

2.2. Light and Electron Microscopy

To observe living cells, an AxioScope A1 light microscope (Carl Zeiss, Jena, Germany) with DIC and phase contrast water immersion objectives ($63\times$ and $100\times$), inverted microscope Axio Observer 5 (Carl Zeiss, Jena, Germany) with DIC and phase contrast (objectives $20\times$), and inverted microscope CKX41 (Olympus, Tokyo, Japan) with phase contrast (objectives $20\times$ and $40\times$) were used. Light microscopic images were taken with a MC-20 camera (Lomo-Microsystems, Saint Petersburg, Russia).

Preparations for studying skeletal elements were carried out as follows. For scanning electron microscopy (SEM), live cells of heliozoans were transferred using a glass micropipette into a small drop of autoclaved mineral water on a coverslip. The drop was air dried after which glass was washed three times with distilled water, air-dried, and attached to the aluminum SEM specimen stub by a conductive carbon adhesive tab (Nisshin EM Co., Ltd., Tokyo, Japan). The preparation was coated with 15 nm gold layer using Auto Fine Coater JFC-1600 (JEOL, Tokyo, Japan) and observed with a JSM-6510LV (JEOL, Tokyo, Japan) electron microscope at an acceleration voltage of 15 kV. For transmission electron microscopy, suspension of live heliozoan cells was transferred onto a formvar-coated copper grids, air-dried, and then washed three times with distilled water. After drying, the preparation was shadowed with tungsten oxide (WO_2) using a JEE-4X vacuum evaporator (JEOL, Tokyo, Japan) and observed with a JEM-1011 (JEOL, Tokyo, Japan) at an acceleration voltage of 80 kV.

Morphological parameters of centrohelids such as cell diameter, spine scale length, basal plate width, marginal rim of basal plate, shaft diameter, height, width and depth of basal plate pockets, plate scales' length and width, length and width of medial thickening of plate scales, and cysts diameter were measured using ImageJ 1.52a [32].

2.3. Molecular Phylogeny

Cells of centrohelid strain HF-25 were grown to high density in a clonal culture and collected by centrifugation ($1000\times g$, room temperature) onto a $0.8\ \mu\text{m}$ -pore membrane of the Vivaclear mini column (Sartorius Stedim Biotech, Stonehouse, UK, VK01P042). Genomic DNA was isolated using the MasterPure™ Complete DNA and RNA Purification Kit (Epicentre, Madison, WI, USA, Cat. No. MC85200). The 18S rRNA gene was amplified using EconoTaq Plus Green $2\times$ Master Mix (Lucigen, Middleton, WI, USA, Cat. No. 30033-1) and universal eukaryotic primers [33]:

GGF (forward): 5'-CTTCGGTCATAGATTAAGCCATGC-3'

GGR (reverse): 5'-CCTTGTTACGACTTCTCCTTCCTC-3'.

The amplification steps are as follows: initial denaturation at 95 °C for 3 min, 35 cycles of 95 °C for 30 s, 52 °C for 30 s, 72 °C for 1.5 min, and a final extension 72 °C for 5 min. Amplified DNA fragments were purified with QIAquick PCR Purification Kit (Qiagen, Hilden, Germany, Cat. No. 433160764). The purified PCR products were then sequenced by Sanger dideoxy sequencing in one replicate using the previously mentioned primers, and two universal internal primers:

18SintF (forward): 5'-GGTAATCCAGCTCCAATAGCGTA-3'

18SintR (reverse): 5'-GTTTCAGCCTTGCGACCATACT-3'.

Seventy-eight centrohelid sequences were retrieved from NCBI GenBank (date of access: 3 November 2021) including all morphologically characterized sequences of *Pterista*, environmental sequences related to strain HF-25, and sequences reflecting the diversity of *Pterista* subclades. All centrohelid sequences were aligned using L-INS-i algorithm in MAFFT version 7.475 [34,35] and trimmed using '-gappypout' method in TrimAl version 1.2 [36]. The resulting alignment consisted of 1491 sites and was used to build the phylogenetic tree (available on figshare <https://doi.org/10.6084/m9.figshare.17113463.v1> (accessed on 7 December 2021)).

To infer Bayesian phylogenetic tree, MrBayes version 3.2.6 [37] was used with four categories of Gamma-distributed among-site rate variation under GTR+I+GAMMA4 substitution model, calculating proportion of invariable sites. To calculate posterior probability, four independent Metropolis-coupled Markov chains were run for 20 million generations, and summarized with a 50% burn-in.

Additionally, maximum likelihood phylogeny was inferred using IQ-TREE v1.6.12 [38] under the best fit model determined by the in-built ModelFinder with and 1000 non-parametric bootstraps.

3. Results

3.1. Cell Morphology of *Triangulopteris lacunata* gen. et sp. nov.

Type Strain: HF-25 (Kolyma Lowland)

A diameter of the starving cells without visible food vacuoles is 4.3–8.5 µm and a length of the axopodia is 5.2–12.7 µm (Figure 2A,D). These starving cells were cultivated for more than two months in a culture with a low number of prey (one prey cell per 40 cells of centrohelids). A diameter of the well-fed cells is 7.23–16.3 µm and a length of the axopodia is 10.9–28.4 µm (Figure 2B,C,E). The ratio of the length of axopodia to the cell diameter is 0.89–2.01 for starving cells and 1.54–2.91 for well-fed heliozoans. Axopodia bear kinetocysts (Figure 3A–D). Cells slowly floated in a water column or crawled on the surface of a Petri dish or attached to a substrate. Colony formation was not observed. A presence of cysts with a diameter of 5.9–7.3 µm was noted for the culture containing starving cells (Figure 2F,G).

The cells are covered with plate scales (Figure 3A,E,F) and spine scales (Figure 3B–D). Spine scales are 1.06–3.33 µm long, have a triangular appearance, consist of a shaft, a basal plate and lateral wings. The shaft is 0.08–0.12 µm wide (Figure 3C), tapering to a sharp apex. The horse hoof-shaped basal plate is 0.60–0.92 µm in diameter (Figure 3C) and surrounded by a small 0.06–0.09 µm wide marginal rim. Two so-called 'pockets' (Figure 3B,D) are located on both sides of the shaft. They are formed by the lateral wings and ends of the hoof-shaped basal plate. Each pocket size is by 0.14–0.36 × 0.07–0.13 µm with a depth of 0.14–0.36 µm. The lateral wings taper from the basal plate to the apex of the shaft (Figure 3B). Radial ribs are located on the inner side of the basal plate and on the lateral wings (Figure 3B). Spine scales are slightly curved distally from the inner part of the basal plate. Plate scales are oval with a size dimension of 1.25–2.05 × 0.86–1.93 µm and its medial thickening with the size 0.47–1.05 × 0.060–0.116 µm (Figure 3E,F).

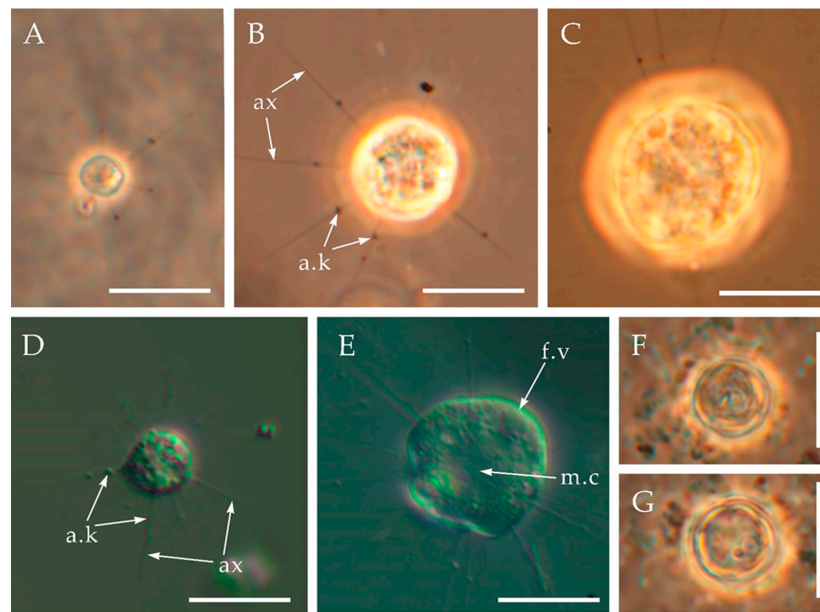


Figure 2. *Triangulopterus lacunata* gen. et sp. nov., strain HF-25 from the Kolyma Lowland after the loss of silica scales, light microscopy. (A,D)—starving cells; (B,C,E)—well-fed cells; (F,G)—cysts. Abbreviations: a.k—axopodial kinetocysts; ax—axopodia; f.v—food vacuole; m.c—microtubule organizing center (MTOC). Scale bars: (A–G)—10 μ m.

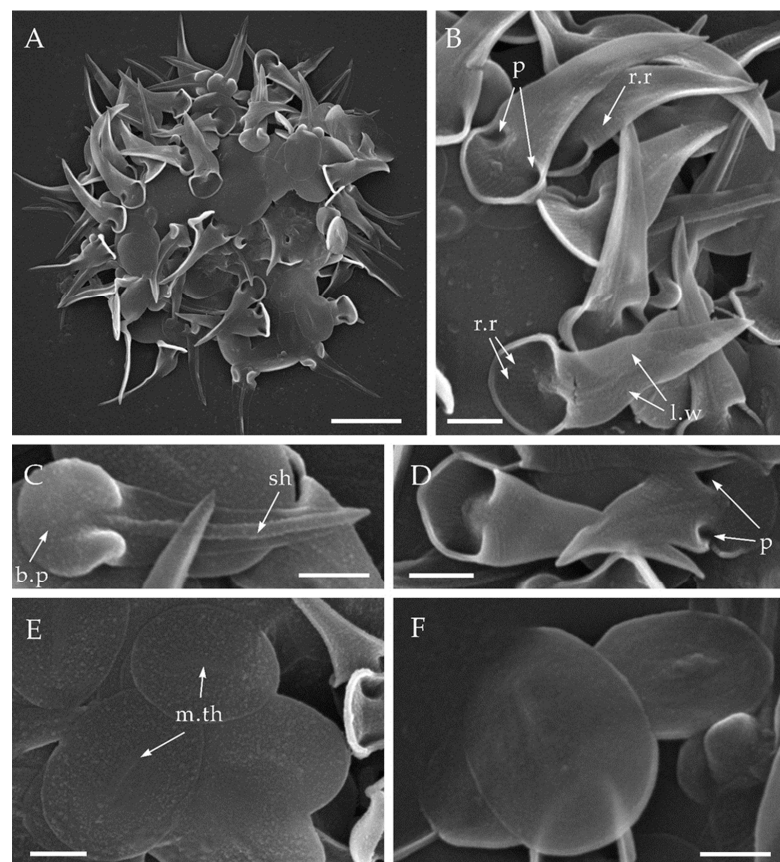


Figure 3. *Triangulopterus lacunata* gen. et sp. nov., strain HF-25 from the Kolyma Lowland, scanning electron microscopy. (A)—general view of the dried cell; (B–D)—spine scales; (E,F)—plate scales. Abbreviations: b.p—basal plate; l.w—lateral wing; m.th—medial thickening; p—pockets; r.r—radial ribs; sh—shaft. Scale bars: (A)—2 μ m; (B–F)—0.5 μ m.

In addition to the type strain HF-25 isolated from the permafrost of the Kolyma Lowland, cells with similar morphology were found in the soil samples from Crimea, an island on the Dnieper River, and in the wet moss with sand from Franz Josef Land archipelago (Figure 4). Comparison of the morphological characteristics of the skeletal elements can be found in Table 2.

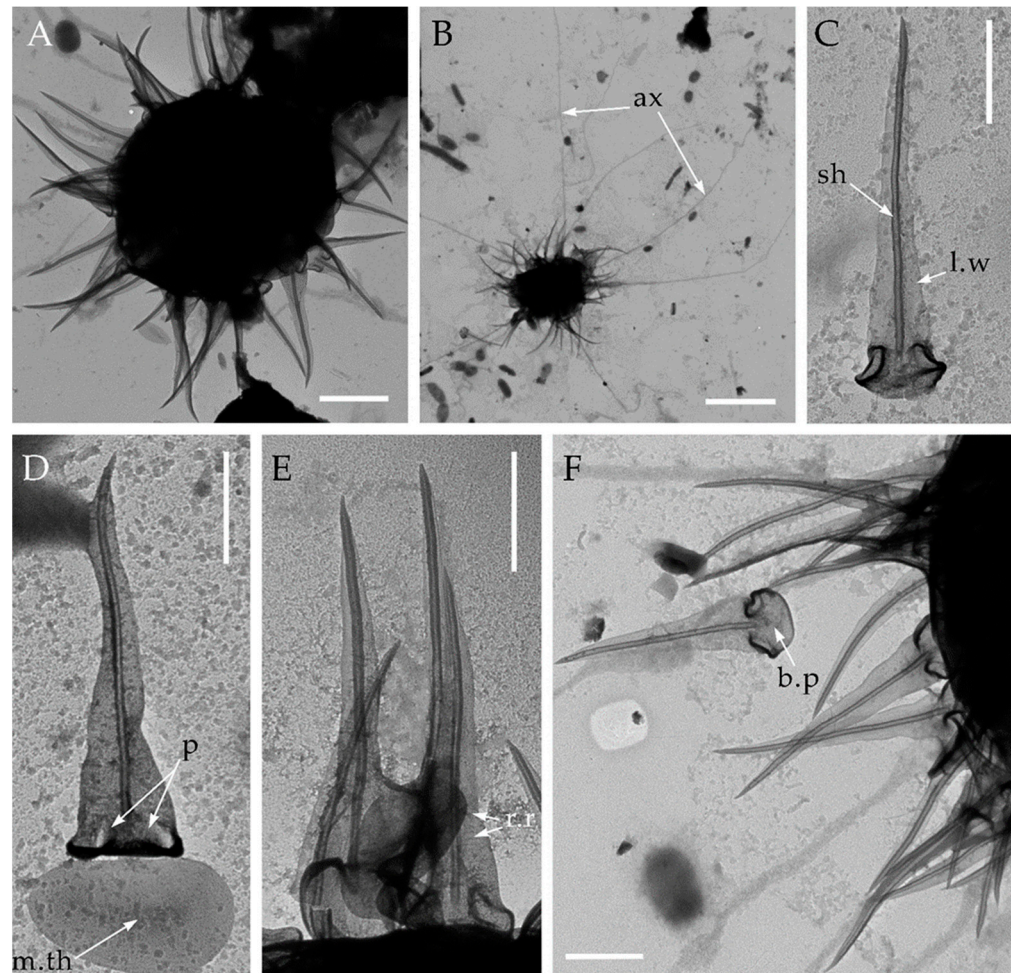


Figure 4. *Triangulopterus lacunata* gen. et sp. nov., from Franz Josef Land archipelago. Electron microscopy (TEM). (A,B)—general view of the dried cell; (C,F)—spine scales; (D,E)—spine and plate scales. Abbreviations: ax—axopodia; b.p—basal plate; l.w—lateral wing; m.th—medial thickening; p—pockets; r.r—radial ribs; sh—shaft. Scale bars: (A)—2 μm ; (B)—5 μm ; (C–F)—1 μm .

3.2. Spicules-Bearing Stage

After several years of cultivating the strain HF-25 using *B. saltans* flagellate as a prey with the addition of rice grains, a loss of silica scales by the HF-25 cells was observed. No silica scales could be observed both in live cell images (Figure 2A–E) and in SEM and TEM images (Figure 5). Instead, irregularly placed needle-shaped spicules (1.85–3.64 μm long and 0.035–0.056 μm wide) were observed in electron microscope over the entire surface of the cells (Figure 5).

3.3. Phylogenetic Analysis

The SSU rRNA based phylogenetic tree recovered the strain HF-25 within the clade Pterista (Figure 6). Strain HF-25 forms a separate lineage in an unresolved trichotomy with the environmental sequence Env H7.1 (AY749492) and the clade H2, consisted of Env H1.10 (AY749488), Env H19.3 (AY749502), Env H5.6 (AY749489), and Env H19.7 (AY749486)

from freshwater biotopes of Botswana, New Zealand, and Singapore. The sequence of HF-25 strain has a rather low similarity with the closest NCBI GenBank sequences from the environment (95.28% with Env H7.1; 92.99% with Env H1.10; 92.99% with H19.3; 95.09% with H5.6; 94.21% with H19.7). The SSU rRNA gene sequence of HF-25 is only 94.08% similar to the closest annotated and morphologically characterized centrohelid, *Pterocystis clarkii* Cavalier-Smith et Von der Heyden, 2007, and even less similar to *Heterophrys miriopoda* (AY749611) and *Sphaerastrum fooskii* (AY749614) from Heterophryidae clade. The latter two species only possess organic spicules covering and are morphologically indistinguishable.

Table 2. Morphological comparison of the skeletal elements of *Triangulopteris lacunata* gen. et sp. nov. from geographically distant biotopes.

Parameter	Kolyma Lowland Strain	Franz Josef Land Strain	Dnieper Lowland Strain	Crimean Strain
Cell diameter, μm	4.3–16.3 (LM) (75)	5.0–6.9 (TEM) (7)	~ 6–7 (SEM) (11)	~ 7 (SEM) (2)
Spine scale length, μm	1.06–3.33 (61)	2.74–4.55 (37)	2.12–4.70 (35)	2.81–4.17 (20)
Basal plate width, μm	0.60–0.92 (52)	0.65–1.17 (26)	0.70–0.90 (29)	0.66–0.91 (19)
Marginal rim of basal plate, μm	0.05–0.07 (31)	0.04–0.05 (7)	0.06–0.09 (25)	0.07–0.09 (5)
Shaft diameter, μm	0.08–0.12 (50)	0.05–0.09 (28)	0.10–0.11 (30)	0.10–0.12 (20)
Pocket height, μm	0.15–0.36 (21)	0.15–0.29 (5)	0.18–0.35 (19)	0.14–0.25 (8)
Pocket width, μm	0.06–0.13 (26)	0.09–0.12 (6)	0.07–0.15 (18)	0.06–0.10 (8)
Pocket depth, μm	0.13–0.36 (15)	0.26 (1)	0.17 (1)	–
Plate scales length, μm	1.25–2.05 (48)	1.76–1.86 (5)	1.22–1.62 (22)	1.63–2.05 (15)
Plate scales width, μm	0.86–1.93 (48)	1.07–1.27 (6)	0.69–0.97 (19)	1.10–1.40 (15)
Length of medial thickening of plate scales, μm	0.47–0.77 (22)	0.82–0.85 (6)	0.72–0.86 (15)	0.59–1.05 (15)
Width of medial thickening of plate scales, μm	0.065–0.116 (18)	0.060–0.064 (6)	0.072–0.085 (12)	0.07–0.15 (15)
Cysts diameter, μm	5.9–7.3 (LM) (20)	–	–	–

(Number of measurements).

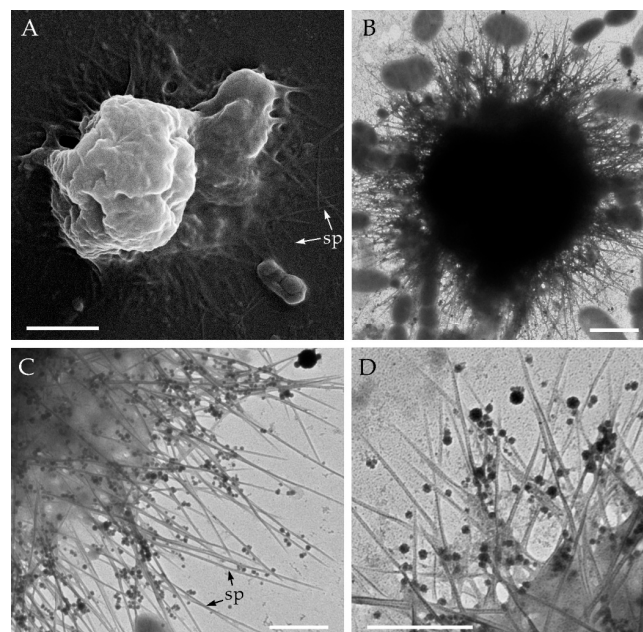


Figure 5. Spicule-bearing stage of *Triangulopteris lacunata* gen. et sp. nov., HF-25 strain from Kolyma Lowland. (A)—general view of the dried cell (SEM); (B)—general view of the dried cell (TEM); (C,D)—spicules on the peripheral part of cells (TEM). Abbreviations: sp—spicules. Scale bars: (A,B)—5 μm ; (C,D)—1 μm .

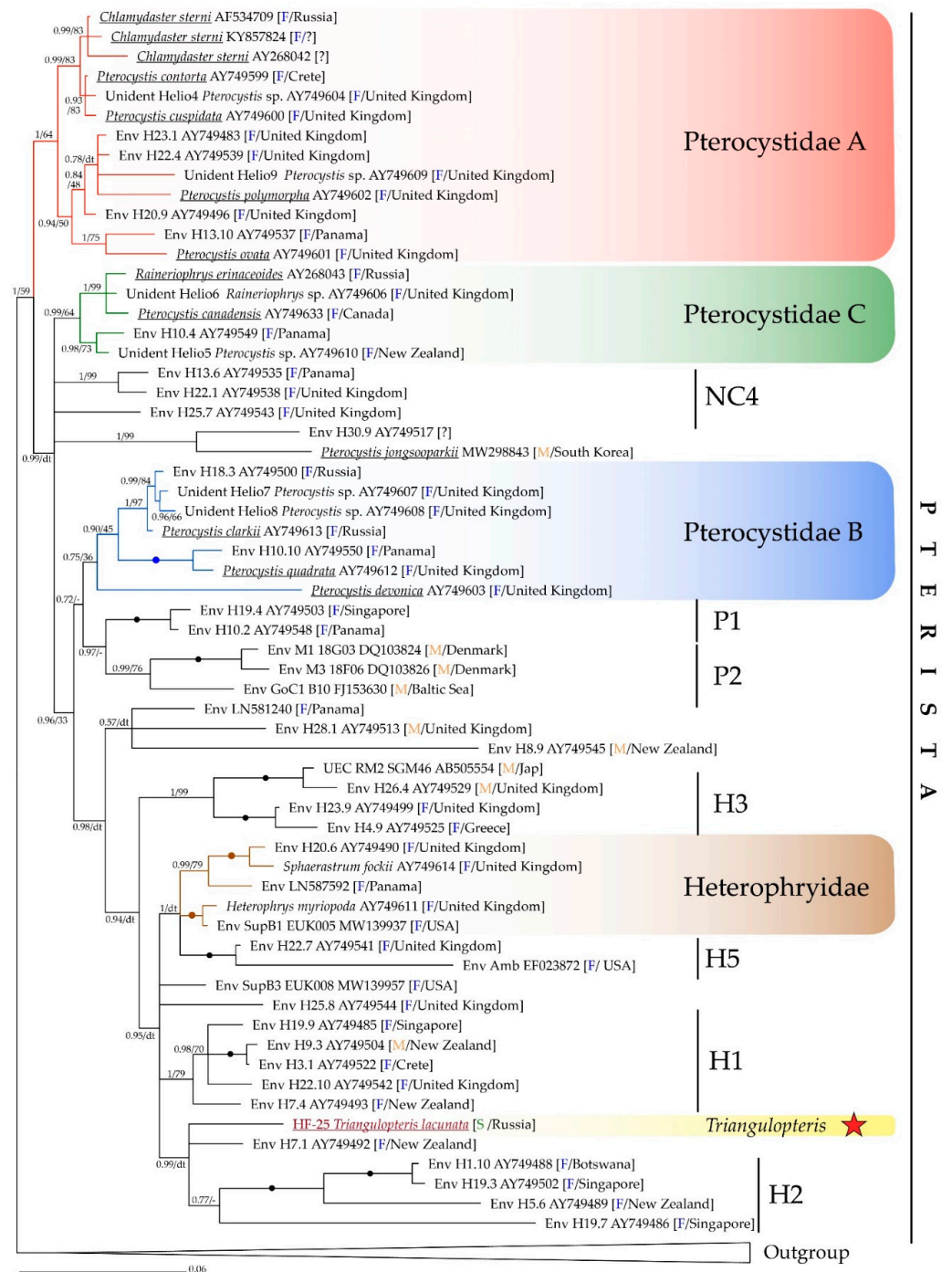


Figure 6. Phylogenetic tree generated from Bayesian analysis based on SSU rRNA gene sequences from 79 centrohelids. The sequence from this study is highlighted in red and marked with a star. Bayesian posterior probabilities (BPP) and Maximum Likelihood (ML, TN+F+R6 model) bootstrap values are indicated on branches (values >0.5/>30 are shown); filled circles indicate values of BPP = 1.00 and ML bootstrap = 100%; dt—different topology. Abbreviations: F—freshwater environment; M—marine environment; S—soil environment. Outgroup: *Clypifer cribrifer* MW700077; *Oxnerella micra* JQ245079; *Meringosphaera mediterranea* MZ240752; *Raphidiophrys drakena* KU178911; *R. heterophryioidea* KU178912; *Yogsothoth knorrus* MH445508; *Pinjata ruminata* MK641802; *Marophrys marina* AF534710; *M. marina* AY268041; *Raphidocystis contractilis* AB196984; *R. ambigua* AF534708; *Acanthocystis nicholli* AY749632; *A. costata* KF990486; *A. amura* KX639994; *Choanocystis symna* KF990487; *Ch. curvata* AY749616; *Spiculophrys aggregata* KU178913.

We propose that the strain HF-25 represents a new genus and species of centrohelid heliozoans due to its isolated placement on the phylogenetic tree and the unique morphology of silica scales.

4. Discussion

Morphological characteristics and the measurements of the newly described centrohelids in this study (Table 2) do not overlap with those of other known centrohelids. Horse hoof-shaped basal plates and triangular lateral wings narrowing toward a sharp apex of clone HF-25 distinguish it from all other centrohelid genera and species except *Raineriophrys scaposa* (Dürschmidt, 1987) Mikrjukov, 2002. The size of the scales, the shape of lateral wings and the basal plates between *R. scaposa* and HF-25 are quite similar. However, the descriptions of *R. scaposa* do not report any structures resembling ‘pockets’ described above. Additionally, no information about the ribs on the surface of the lateral and basal wings are recounted. Such distinctive features are not visualized on the microphotographs in the original description either [39]. Another *R. scaposa* described in the work of Wujek [40], also lacks characteristic features described in spine scales of our strain. It is noteworthy that *Raineriophrys scaposa* was first described as *Acanthocystis scaposa*, from samples obtained from freshwater in Chile and Sri Lanka [39]. Later it was transferred to the genus *Pterocystis* [6], and then to *Raineriophrys* [1].

To this day, NCBI GenBank contains merely one sequence of *Raineriophrys* which was morphologically identified. *Raineriophrys erinaceoides* (type species of the genus *Raineriophrys*) belongs to the clade Pterocystida C together with *Pterocystis canadensis* (AY749633). The problems associated with SSU rRNA sequences belonging to Pterocystida C clade were discussed previously [27], one of which is that the two similar sequences (98.86%), *P. canadensis* (AY749633) and *R. erinaceoides* (AY268043) are assigned to different genera. Considering the morphology of the skeletal elements of *T. lacunata* and *R. scaposa* is similar to some extent, we assume that they are representatives of the same genus. It would be necessary to obtain molecular data on *R. scaposa* to resolve this ambiguity. The presence of horse hoof-shaped basal plates, triangular lateral wings narrowing to the sharp apex, and isolated phylogenetic position of clone HF-25 distant from the type species of the genus *Raineriophrys*, allow us to consider it a member of a new genus.

The morphological characteristics of four *T. lacunata* strains from geographically distant biotopes are very similar. Interestingly, *T. lacunata* was found in several soil samples at once and has never been found in freshwater bodies. Apparently, this organism is a representative of specific soil microbial ecosystems. Soils and temporary shallow freshwater biotopes remain poorly explored [41–44]. The information about centrohelid heliozoans from soils is especially scanty. No special studies have been conducted. There are only a few works that mention centrohelids in soil samples [12,13]. However, growing metabarcoding studies have just started to unveil new and intriguing information about the soil-associated protist communities including centrohelids. For example, Singer et al. [15], have shown that species diversity of soil protists is more numerous than that of both marine and freshwater: the number of operating taxonomic units (OTUs) assigned to centrohelids in soils is twice as much as the ones in freshwater biotopes and 10 times higher than that of marine waters.

A metatranscriptomic study of protists of soil systems in Europe [14] revealed the presence of centrohelids with relative abundance of SSU rRNA sequences up to 1%. Thus, centrohelid heliozoans are diverse and ubiquitous component of soil microbial communities.

Two strains of centrohelid studied here were isolated from frozen soil and peat. It has been known that protists can remain viable at permafrost conditions for hundreds to hundreds of thousands of years [13,45–50]. The discovery of a centrohelid heliozoan in the permafrost of the Kolyma River basin was reported earlier [13]: viable cysts of a heliozoan, identified as *Choanocystis perpusilla* (Petersen et Hansen, 1960) Siemensma, 1991, were isolated from sediments of the Late Pleistocene fossil burrows of ground squirrels [13]. In our study, centrohelid heliozoans were found in two sites near Cape Maliy Chukochiy: (1) buried peat from a depth of 35–40 cm; (2) mineral soil from a depth of 60–65 cm,

both of which are layers belonging to Holocene deposits. The average thickness of active layer of the permafrost in Cape Maliy Chukochiy is 42 cm, but in some years, it can go up to 64 cm [51]. The isolated strains of *T. lacunata* gen. et sp. nov. and their locations complement our knowledge of paleoprotists. It should be noted that at present there is an increase in the thickness of active permafrost layer and thawing of permafrost leading to a change in the ecological balance and composition of microbial communities [52–54].

We observed that *T. lacunata* gen. et sp. nov. cells lose silica scales in the studied old cultures and produce radial needle-shaped spicules. A similar change in the type of scales is shown for *Raphidocystis glabra* Dürschmidt 1985 [7]. The stages of a complex life cycle are described in detail for *Raphidiophrys heterophryoidea* Zlatogursky, 2012, and at a certain stage, it has been described to possess organic spicules [8,20]. A similar change of cells covers is therefore, a likely typical character for other genera.

Here we present the third confirmed case of silica scales being replaced to spicules. It is also highly unlikely a contamination as the two monoclonal cultures were isolated from the samples from the adjacent collection points. Morphology of cells from both cultures were visualized using electron microscopy and silica scales were noted. SSU rRNA genes of both cultures were also sequenced (the sequence identity was 99.9%). A few years later, a change to spicule-bearing stage was found in both cultures.

Strains of *T. lacunata* studied here were isolated from geographically distant biotopes (Figure 1). Global distribution of centrohelids and some other protists have already been reported [1,44]. The five most closely related environmental sequences (Figure 5) are also obtained from remote freshwater locations in Botswana, New Zealand, and Singapore. However, the factors influencing centrohelid diversity and distribution remain unclear. More research is needed to understand the relationships within the different phylogenetic clades of centrohelids and boundaries of their main taxa. It is also necessary to sequence more SSU rRNA genes and thoroughly investigate the morphology of skeletal elements of closely related strains of centrohelids, including those from poorly studied soil biotopes.

Taxonomic Summary

DIAPHORETICKES Adl et al., 2012

- Haptista Cavalier-Smith, 2003
- Centroplasthelida Febvre-Chevalier et Febvre, 1984
- Pterocystida Cavalier-Smith et von der Heyden, 2007
- Pterista Shishkin et Zlatogursky, 2018
- Pterocystidae Cavalier-Smith et von der Heyden, 2007

Triangulopteris Zagumyonnyi, Radaykina and Tikhonenkov gen. nov.

Diagnosis: Centrohelid heliozoans with two types of silica covering elements. Spine scales have a triangular appearance, they consist of a hoof-shaped basal plate, a hollow pointed shaft, and lateral wings tapering to sharp apex. Plate scales are oval, smooth, with a poorly developed medial thickening.

Type species: *Triangulopteris lacunata* sp. nov.

Etymology: From Latin “triangulus”—triangular and from Greek “πτερόν”—wing; due to the shape of spine scales, which has a triangular appearance.

ZooBank Registration: <http://zoobank.org/NomenclaturalActs/01EB060E-9DC7-49CF-99CE-71FED936B6F2> (accessed on 7 December 2021)

Triangulopteris lacunata Zagumyonnyi, Radaykina and Tikhonenkov sp. nov.

Diagnosis: Cell diameter ranges between 4.3–16.3 µm. Spine scales are 1.06–4.70 µm long, have a triangular appearance; shaft is 0.05–0.12 µm in diameter, hoof-shaped basal plate is 0.60–1.17 µm in diameter; lateral wings taper from the basal plate to the apex of the shaft; two ‘pockets’ are located on both sides of the shaft; radial ribs are located on the inner side of the basal plate and on the lateral wings. Plate scales are oval, 1.22–2.05 × 0.69–1.93 µm with medial thickening of 0.47–1.05 × 0.060–0.116 µm. Cysts with a diameter of 5.9–7.3 µm. Siliceous scales can be completely lost and replaced by organic 1.85–3.64 µm long spicules.

Etymology: From Latin “lacuna”—hole, fossa; due to the presence of two ‘pockets’ formed at the transition of the lateral wings to the basal plate.

Hapantotype: Air-dried preparations for SEM No. 2-HF-25 is kept in the laboratory of Microbiology at the Papanin Institute for Biology of Inland Waters RAS (Borok, Russia).

Gene sequence: The SSU rRNA gene sequence has the GenBank Accession Number OL739463.

ZooBank Registration: <http://zoobank.org/NomenclaturalActs/4B2D297B-9C53-4160-A49F-79690BEE5719> (accessed on 7 December 2021)

Type strain: HF-25. Stored in the collection of live protozoan cultures at IBIW RAS.

Type Figure: Figure 3A–E.

Type locality: Fluvial terraces of the mouth of the Bolshaya Chukochya river, Kolyma Lowland, North-Eastern Siberia (70°03′53.9″ N 159°44′06.6″ E)

Habitat: Soil of dry stream from Syuryu-Kaya Mt, Crimean Peninsula; soil and willow leaf litter from Pesiv Island, Dnieper River, East European Plain; moss with sand in the glacier melting zone from Champ Island (Franz Josef Land archipelago, Arctic Ocean); buried peat, cryoturbated and mineral soils of Cape Maliy Chukochiy vicinity, Kolyma Lowland (North-Eastern Siberia).

Author Contributions: Conceptualization, D.G.Z., D.V.T.; methodology, D.G.Z., L.V.R.; formal analysis, D.G.Z.; investigation, D.G.Z., L.V.R., D.V.T.; resources, D.V.T.; writing—original draft preparation, D.G.Z., D.V.T.; writing—review and editing, L.V.R., D.V.T.; visualization, D.G.Z.; supervision, D.V.T.; funding acquisition, D.V.T. All authors have read and agreed to the published version of the manuscript.

Funding: This research was funded by the Tyumen Oblast Government, as part of the West-Siberian Interregional Science and Education Center’s project No. 89-DON (2).

Institutional Review Board Statement: Not applicable.

Informed Consent Statement: Not applicable.

Data Availability Statement: Not applicable.

Acknowledgments: We thank Mylnikov A.P., Shatilovich A.V., Gubin S.V., Lupachev A.V., Budaev V.N., Budaeva I.A. and Dubrovsky Y.V. for soil samples. We are grateful to Anna Cho (University of British Columbia) for editing the English language.

Conflicts of Interest: The authors declare no conflict of interest. The funders had no role in the design of the study; in the collection, analyses, or interpretation of data; in the writing of the manuscript, or in the decision to publish the results.

References

1. Mikrjukov, K.A. *Centrohelid Heliozoans (Centroheliocystis)*; KMK Scientific Press: Moscow, Russia, 2002; 136p.
2. Burki, F.; Kaplan, M.; Tikhonenkov, D.V.; Zlatogursky, V.; Minh, B.Q.; Radaykina, L.V.; Smirnov, A.; Mylnikov, A.P.; Keeling, P.J. Untangling the early diversification of eukaryotes: A phylogenomic study of the evolutionary origins of Centrohelida, Haptophyta and Cryptista. *Proc. R. Soc. B* **2016**, *283*, 20152802. [[CrossRef](#)]
3. Bardele, C.F. The fine structure of the centrohelidian heliozoan *Heterophrys marina*. *Cell Tissue Res.* **1975**, *161*, 85–102. [[CrossRef](#)] [[PubMed](#)]
4. Bardele, C.F. Comparative study of axopodial microtubule patterns and possible mechanisms of pattern control in the centrohelidian heliozoa *Acanthocystis*, *Raphidiophrys* and *Heterophrys*. *J. Cell Sci.* **1977**, *25*, 205–232. [[CrossRef](#)] [[PubMed](#)]
5. Febvre-Chevalier, C.; Febvre, J. Axonemal microtubule pattern of *Cienkowskya mereschkovskiyi* and a revision of heliozoan taxonomy. *Orig. Life* **1984**, *13*, 315–338. [[CrossRef](#)]
6. Siemensma, F.J. Klasse Heliozoa Haeckel, 1866. In *Nackte Rhizopoda und Heliozoa. Protozoenfauna, Bd 2*; Gustav Fischer Verlag, Stuttgart: New York, NY, USA, 1991; pp. 171–297.
7. Zlatogursky, V.V.; Drachko, D.; Klimov, V.I.; Shishkin, Y. On the phylogenetic position of the genus *Raphidocystis* (Haptista: Centroplasthelida) with notes on the dimorphism in centrohelid life cycle. *Eur. J. Protistol.* **2018**, *64*, 82–90. [[CrossRef](#)]
8. Drachko, D.; Shishkin, Y.; Zlatogursky, V.V. Phenotypic masquerade: Polymorphism in the life cycle of the centrohelid heliozoan *Raphidiophrys heterophryoidea* (Haptista: Centroplasthelida). *Eur. J. Protistol.* **2020**, *73*, 125686. [[CrossRef](#)] [[PubMed](#)]
9. Cavalier-Smith, T.; Chao, E.E. *Oxnerella micra* sp. n. (Oxnerellidae fam. n.), a tiny naked centrohelid, and the diversity and evolution of heliozoan. *Protist* **2012**, *163*, 574–601. [[CrossRef](#)] [[PubMed](#)]

10. Cavalier-Smith, T.; von der Heyden, S. Molecular phylogeny, scale evolution and taxonomy of centrohelid heliozoan. *Mol. Phylogenet. Evol.* **2007**, *44*, 1186–1203. [[CrossRef](#)]
11. Triadó-Margarit, X.; Casamayor, E.O. High genetic diversity and novelty in planktonic protists inhabiting inland and coastal high salinity water bodies. *FEMS Microbiol. Ecol.* **2013**, *85*, 27–36. [[CrossRef](#)]
12. Gerasimova, E.A.; Plotnikov, A.O.; Khlopko, Y.A.; Zlatogursky, V.V. Multiple euryhaline lineages of centrohelids (Haptista: Centroplasthelida) in inland saline waters revealed with metabarcoding. *J. Eukaryot. Microbiol.* **2020**, *67*, 223–231. [[CrossRef](#)]
13. Shatilovich, A.V.; Mylnikov, A.P.; Stoupin, D.V. The fauna and morphology of heterotrophic flagellates and heliozoans from Late Pleistocene fossil rodent burrows (Kolyma Lowland). *Zool. Zhurn.* **2010**, *89*, 387–397, (In Russian with English summary).
14. Geisen, S.; Tveit, A.T.; Clark, I.M.; Richter, A.; Svenning, M.M.; Bonkowski, M.; Urich, T. Metatranscriptomic census of active protists in soils. *ISME J.* **2015**, *9*, 2178–2190. [[CrossRef](#)] [[PubMed](#)]
15. Singer, D.; Seppely, C.V.W.; Lentendu, G.; Dunthorn, M.; Bass, D.; Belbahri, L.; Blandenier, Q.; Debroas, D.; de Groot, G.A.; de Vargas, C.; et al. Protist taxonomic and functional diversity in soil, freshwater and marine ecosystems. *Environ. Int.* **2021**, *146*, 106262. [[CrossRef](#)]
16. Leonov, M.M. New species of centrohelid heliozoa of the genus *Acanthocystis* (Centroheliozoa). *Zool. Zhurn.* **2010**, *89*, 507–513, (in Russian with English summary).
17. Leonov, M.M.; Mylnikov, A.P. Centroheliozoa from Southern Karelia. *Zool. Zhurn.* **2012**, *91*, 515–523, (In Russian with English summary).
18. Tikhonenkov, D.V.; Mylnikov, A.P. *Choanocystis antarctica* sp. n., a new heliozoan (Centrohelida) species from the littoral zone of King George Island, South Shetland Islands, Antarctica. *Biol. Bull.* **2011**, *38*, 663–666. [[CrossRef](#)]
19. Zlatogursky, V.V. Three new freshwater species of centrohelid heliozoans: *Acanthocystis crescenta* sp. nov., *A. kirilli* sp. nov., and *Choanocystis minima* sp. nov. *Eur. J. Protistol.* **2010**, *46*, 159–163. [[CrossRef](#)] [[PubMed](#)]
20. Zlatogursky, V.V. *Raphidiophrys heterophryioidea* sp. nov. (Centrohelida: Raphidiophryidae), the first heliozoan species with a combination of siliceous and organic skeletal elements. *Eur. J. Protistol.* **2012**, *48*, 9–16. [[CrossRef](#)]
21. Zlatogursky, V.V. Two new species of centrohelid heliozoans: *Acanthocystis costata* sp. nov. and *Choanocystis symna* sp. nov. *Acta Protozool.* **2014**, *53*, 313–324.
22. Zlatogursky, V.V.; Gerasimova, E.A.; Plotnikov, A.O. A new species of centrohelid heliozoan *Acanthocystis amura* n. sp. isolated from two remote locations in Russia. *J. Eukaryot. Microbiol.* **2017**, *64*, 434–439. [[CrossRef](#)] [[PubMed](#)]
23. Zlatogursky, V.V.; Gerasimova, E.A.; Drachko, D.; Klimov, V.I.; Shishkin, Y.; Plotnikov, A.O. *Pinjata ruminata* gen. et sp. n.—A new member of centrohelid family Yogsothothidae (Haptista: Centroplasthelida) from the brackish river. *J. Eukaryot. Microbiol.* **2019**, *66*, 862–868. [[CrossRef](#)]
24. Gerasimova, E.A.; Plotnikov, A.O. New freshwater species of centrohelids *Acanthocystis lyra* sp. nov. and *Acanthocystis siemensmae* sp. nov. (Haptista, Heliozoa, Centrohelea) from the South Urals, Russia. *Acta Protozool.* **2016**, *55*, 231–237.
25. Prokina, K.I.; Zagumyonnyi, D.G.; Mylnikov, A.P. Marine Centrohelid heliozoans (Centroplasthelida Febvre-Chevalier et Febvre, 1984) from bays of Sevastopol (The Black Sea shore). *Russ. J. Mar. Biol.* **2019**, *45*, 377–384. [[CrossRef](#)]
26. Prokina, K.I.; Radaykina, L.V.; Mylnikov, A.P. Centrohelid Heliozoans (Centroplasthelida Febvre-Chevalier et Febvre 1984) from Vietnam. *Biol. Bull.* **2020**, *47*, 29–40. [[CrossRef](#)]
27. Zagumyonnyi, D.G.; Prokina, K.I.; Tikhonenkov, D.V. First findings of centrohelid heliozoans (Haptista: Centroplasthelida) from marine and freshwater environments of South Korea. *Protistology* **2020**, *14*, 227–245. [[CrossRef](#)]
28. Shishkin, Y.; Drachko, D.; Zlatogursky, V.V. *Clypifer cribrifer* gen. nov., sp. nov. (Clypiferidae fam. nov., Pterocystida, Centroplasthelida), with notes on evolution of centrohelid siliceous coverings. *Int. J. Syst. Evol. Microbiol.* **2021**, *71*. [[CrossRef](#)] [[PubMed](#)]
29. Drachko, D.; Mikhailovskii, V.; Shishkin, Y.; Zlatogursky, V.V. Phylogenetic position and morphology of *Raphidiophrys elongata* sp. nov. (Haptista: Centroplasthelida) with notes on cyst wall structure and evolution. *Eur. J. Protistol.* **2021**, *81*, 125836. [[CrossRef](#)] [[PubMed](#)]
30. Prokina, K.I.; Zagumyonnyi, D.G.; Tikhonenkov, D.V. Centrohelid heliozoans (Centroplasthelida Febvre-Chevalier et Febvre, 1984) from different types of freshwater bodies in the Middle Russian forest-steppe. *Acta Protozool.* **2018**, *57*, 243–266. [[CrossRef](#)]
31. Vørs, N. Heterotrophic amoebae, flagellates and Heliozoa from the Tvärminne area, Gulf of Finland, in 1988–1990. *Ophelia* **1992**, *36*, 1–109. [[CrossRef](#)]
32. Schneider, C.A.; Rasband, W.S.; Eliceiri, K.W. NIH Image to ImageJ: 25 years of image analysis. *Nat. Methods* **2012**, *9*, 671–675. [[CrossRef](#)]
33. Gile, G.H.; James, E.R.; Scheffrahn, R.H.; Carpenter, K.J.; Harper, J.T.; Keeling, P.J. Molecular and morphological analysis of the family Calonymphidae with a description of *Calonympha chia* sp. nov., *Snyderella kirbyi* sp. nov., *Snyderella svezyae* sp. nov. and *Snyderella yamini* sp. nov. *Int. J. Syst. Evol. Microbiol.* **2011**, *61*, 2547–2558. [[CrossRef](#)] [[PubMed](#)]
34. Katoh, K.; Kuma, K.; Toh, H.; Miyata, T. MAFFT version 5: Improvement in accuracy of multiple sequence alignment. *Nucleic Acids Res.* **2005**, *33*, 511–518. [[CrossRef](#)] [[PubMed](#)]
35. Katoh, K.; Standley, D.M. MAFFT multiple sequence alignment software version 7: Improvements in performance and usability. *Mol. Biol. Evol.* **2013**, *30*, 772–780. [[CrossRef](#)] [[PubMed](#)]
36. Capella-Gutierrez, S.; Silla-Martinez, J.M.; Gabaldon, T. TrimAl: A tool for automated alignment trimming in large-scale phylogenetic analyses. *Bioinformatics* **2009**, *25*, 1972–1973. [[CrossRef](#)]

37. Ronquist, F.; Huelsenbeck, J.P. MrBayes 3: Bayesian phylogenetic inference under mixed models. *Bioinformatics* **2003**, *19*, 1572–1574. [[CrossRef](#)]
38. Nguyen, L.T.; Schmidt, H.A.; Haeseler, A.; Minh, B.Q. IQ-TREE: A fast and effective stochastic algorithm for estimating maximum likelihood phylogenies. *Mol. Biol. Evol.* **2015**, *32*, 268–274. [[CrossRef](#)] [[PubMed](#)]
39. Dürschmidt, M. An electron microscopical study of freshwater Heliozoa (genus *Acanthocystis*, Centrohelidia) from Chile, New Zealand, Malaysia and Sri Lanka. II. *Arch. Protistenkunde.* **1987**, *133*, 21–48. [[CrossRef](#)]
40. Wujek, D.E. Freshwater heliozoa from Florida. *Fla. Sci.* **2006**, *69*, 177–191.
41. Simon, M.; López-García, P.; Deschamps, P.; Moreira, D.; Restoux, G.; Bertolino, P.; Jardillier, L. Marked seasonality and high spatial variability of protist communities in shallow freshwater systems. *ISME J.* **2015**, *9*, 1941–1953. [[CrossRef](#)]
42. Simon, M.; Jardillier, L.; Deschamps, P.; Moreira, D.; Restoux, G.; Bertolino, P.; López-García, P. Complex communities of small protists and unexpected occurrence of typical marine lineages in shallow freshwater systems. *Environ. Microbiol.* **2015**, *17*, 3610–3627. [[CrossRef](#)] [[PubMed](#)]
43. Geisen, S.; Mitchell, E.A.D.; Adl, S.; Bonkowski, M.; Dunthorn, M.; Ekelund, F.; Fernández, L.D.; Jousset, A.; Krashevskaya, V.; Singer, D.; et al. Soil protists: A fertile frontier in soil biology research. *FEMS Microbiol. Rev.* **2018**, *42*, 293–323. [[CrossRef](#)]
44. Oliverio, A.M.; Geisen, S.; Delgado-Baquerizo, M.; Maestre, F.T.; Turner, B.L.; Fierer, N. The global-scale distributions of soil protists and their contributions to belowground systems. *Sci. Adv.* **2020**, *6*, eaax8787. [[CrossRef](#)]
45. Shatilovich, A.V.; Shmakova, L.A.; Mylnikov, A.P.; Gilichinsky, D.A. Ancient Protozoa isolated from permafrost. In *Permafrost Soils*; Margesin, R., Ed.; Springer: Berlin/Heidelberg, Germany, 2009; pp. 97–115.
46. Stoupin, D.; Kiss, A.K.; Arndt, H.; Shatilovich, A.V.; Gilichinsky, D.A.; Nitsche, F. Cryptic diversity within the choanoflagellate morphospecies complex *Codosiga botrytis*—phylogeny and morphology of ancient and modern isolates. *Eur. J. Protistol.* **2012**, *48*, 263–273. [[CrossRef](#)]
47. Shmakova, L.A.; Rivkina, E.M. Viable eukaryotes of the phylum Amoebozoa from the Arctic permafrost. *Paleontol. J.* **2015**, *49*, 572–577. [[CrossRef](#)]
48. Shatilovich, A.; Stoupin, D.; Rivkina, E. Ciliates from ancient permafrost: Assessment of cold resistance of the resting cysts. *Eur. J. Protistol.* **2015**, *51*, 230–240. [[CrossRef](#)] [[PubMed](#)]
49. Shmakova, L.; Bondarenko, N.; Smirnov, A. Viable species of *Flamella* (Amoebozoa: Variosea) isolated from ancient arctic permafrost sediments. *Protist* **2016**, *167*, 13–30. [[CrossRef](#)]
50. Malavin, S.; Shmakova, L.; Claverie, J.-M.; Rivkina, E. Frozen Zoo: A collection of permafrost samples containing viable protists and their viruses. *Biodivers. Data J.* **2020**, *8*, e51586. [[CrossRef](#)]
51. Fyodorov-Davydov, D.G.; Kholodov, A.L.; Ostroumov, V.E.; Kraev, G.N.; Sorokovikov, V.A.; Davydov, S.P.; Merkalova, A.A. Seasonal thaw of soils in the North Yakutian ecosystems. In Proceedings of the 9th International Conference on Permafrost, Fairbanks, AK, USA, 29 June–3 July 2008; Kane, D.L., Hinkel, K.M., Eds.; Institute of Northern Engineering, University of Alaska: Fairbanks, AK, USA, 2008; pp. 481–486. [[CrossRef](#)]
52. Biskaborn, B.K.; Smith, S.L.; Noetzel, J.; Matthes, H.; Vieira, G.; Streletskiy, D.A.; Schoeneich, P.; Romanovsky, V.E.; Lewkowicz, A.G.; Abramov, A.; et al. Permafrost is warming at a global scale. *Nat. Commun.* **2019**, *10*, 264. [[CrossRef](#)] [[PubMed](#)]
53. Inglese, C.N.; Christiansen, C.T.; Lamhonwah, D.; Moniz, K.; Montross, S.N.; Lamoureux, S.; Lafrenière, M.; Grogan, P.; Walker, V.K. Examination of soil microbial communities after permafrost thaw subsequent to an active layer detachment in the high Arctic. *Arct. Antarct. Alp. Res.* **2017**, *49*, 455–472. [[CrossRef](#)]
54. Wu, M.-H.; Chen, S.-Y.; Chen, J.-W.; Xue, K.; Chen, S.-L.; Wang, X.-M.; Chen, T.; Kang, S.C.; Rui, J.P.; Thies, J.E.; et al. Reduced microbial stability in the active layer is associated with carbon loss under alpine permafrost degradation. *PNAS* **2021**, *118*, e2025321118. [[CrossRef](#)] [[PubMed](#)]